Self-healable organic electrochemical transistor with high transconductance, fast response and long-term stability

Journal:	*ACS Applied Materials & Interfaces*
Manuscript ID	am-2020-079137.R1
Manuscript Type:	Article
Date Submitted by the Author:	n/a
Complete List of Authors:	Ko, Jieun; Nanyang Technological University, School of Electrical and Electronic Engineering Wu, Xihu; Nanyang Technological University, School of Electrical and Electronic Engineering Surendran, Abhijith; Nanyang Technological University, School of Electrical and Electronic Engineering Muhammad, Bening ; Nanyang Technological University, School of Electrical and Electronic Engineering Leong, Wei Lin; Nanyang Technological University, School of Electrical and Electronic Engineering

Self-healable Organic Electrochemical Transistor with High Transconductance, Fast Response and Long-term Stability

*Jieun Ko†, Xihu Wu†, Abhijith Surendran, Bening Tirta Muhammad and Wei Lin Leong**

Dr. J. Ko, X. Wu, A. Surendran, Prof. W. L. Leong
School of Electrical Electronic Engineering, Nanyang Technological University, 50 Nanyang Avenue, Singapore 639798, Singapore
E-mail: wlleong@ntu.edu.sg

B. T. Muhammad
Interdisciplinary Graduate School, Nanyang Technological University, 50 Nanyang Avenue, Singapore 639798, Singapore

†These authors contributed equally to this work.

KEYWORDS: organic electrochemical transistors, self-healable electronics, PEDOT:PSS, organic mixed conductors, bioelectronics, flexible electronics

Abstract

The major challenges in developing self-healable conjugated polymers for organic electrochemical transistors (OECTs) lie in maintaining good mixed electronic/ionic transport and the need for fast restoration to the original electronic and structural properties after the self-healing process. Herein, we provide the first report of an all solid state OECT that is self-healable and possess good electrical performance, by utilizing a matrix of poly(3,4-ethylenedioxythiophene):poly(styrenesulfonate) (PEDOT:PSS) and non-ionic surfactant, Triton X-100 as channel, and ion conducting poly(vinyl alcohol) hydrogel as a quasi-solid-state polymer electrolyte. The fabricated OECT exhibits high transconductance (maximum 54 mS), on/off current ratio of ~1.5×10^3, fast response time of 6.8 ms and good operational stability after 68 days of storage. Simultaneously, the OECT showed remarkable self-healing and ion-sensing behaviors and recovered ~95% of its ion sensitivity after healing. These findings will contribute to the development of high performing and robust OECTs for wearable bioelectronic devices.

INTRODUCTION

The use of conjugated polymers for bioelectronics applications is especially attractive due to their favorable properties, namely, chemical stability, facile processability, biocompatibility, electronic and ionic transport as well as enabling an amiable interface with living cells and tissues.[1–5] One new class of devices that leverage these many attributes of conjugated polymers is organic electrochemical transistors (OECTs). In OECT, ions from an electrolyte penetrate a conjugated polymer network and modulate the conductivity through intricate ion-electron coupling.[6] Owing to their high transconductance and thus capable of amplifying small chemical signals with high sensitivity, OECTs are especially promising for diverse biomedical applications such as the detection of ions[7,8], metabolites[9,10], alcohol[11], DNA[12,13], and cells[14–16]. Additionally, they can be fabricated by facile solution and printing processes that allow low cost and large area fabrication.

Poly(3,4-ethylenedioxythiophene):poly(styrenesulfonate) (PEDOT:PSS) has been extensively used as OECT channel layer and demonstrated outstanding transconductance values.[17,18] The OECT performances are influenced by the combination of charge transport in PEDOT chains and volumetric doping in the whole channel area. Although the exact requirements for the ideal morphology for OECT performance still warrants further investigation, it is clear that there is a trade-off between a highly ordered polymer chain for high conductivity and loose packing for sufficient hydration that allows ion penetration.[19–21] To enhance the electrical performance of PEDOT:PSS based OECT systems, various additives such as ethylene glycol[19] and ionic liquids[22–24] have been considered to lead reorganization of PEDOT domain. Especially, the addition of ionic liquid in PEDOT:PSS contributes to form a fibrillar PEDOT network thereby obtaining both high transconductance and fast transient response in the OECT device.[22] This is

because the strong molecular interaction between PEDOT:PSS and ionic liquid allows the molecular rearrangement of PEDOT:PSS[22,25] and the morphology can be tuned by changing the cation or anions of the ionic liquid. Therefore, the introduction of appropriate additives in PEDOT:PSS is a good strategy to develop a high performance OECT device.

More recently, there is a growing demand for wearable and body-integrated implantable sensors.[1,26–28] To enhance the practicality of employing OECTs in smart and wearable devices, it is also desirable to look at active materials with good flexibility and durability to withstand wear, scratching, and unexpected damage from mechanical bending. In particular, the highly crystalline PEDOT required for good electronic properties are often rigid and vulnerable to strain (≈6% fracture strain).[29] There have been efforts to improve the mechanical properties of PEDOT:PSS. For instance, the addition of plasticizers, elastomeric materials such as polydimethylsiloxane and surfactants such as zonyl and triton in PEDOT:PSS serve to improve the stretchability but typically reduce the conductivity.[30–32] Another promising strategy is the use of ionic liquids in PEODT:PSS to induce the formation of nanofibrillar-like structures to improve the stretchability.[22,25] However, the strong molecular interactions between PEDOT:PSS and ionic liquid also induce solution gelation and affect the film processability. The ability of electronic materials to self-heal autonomously like living tissues is an interesting approach to fabricate devices with high reliability and longer lifetime. However, the application of self-healing materials for OECTs remains largely unexplored and the first report was demonstrated through water-enabled healing of PEDOT:PSS.[33] The major challenges in developing such self-healable conjugated polymers for OECTs lie in maintaining good electronic, ionic transport and mechanical properties simultaneously as well as the need for fast restoration to the original electronic and structural properties after the self-healing process.

Among the various additive strategies, the incorporation of a non-ionic surfactant, Triton X-100 in PEDOT:PSS (Figure S1, in the Supporting Information) has been shown to aid in the formation of PEDOT nanofibrils and increases the electrical conductivity of PEDOT:PSS.[32] Another effect of Triton X-100 is that it behaves as healing agent as it enhances the polymer chain mobility and thus improves the viscoelastic properties of PEDOT:PSS film.[34,35] However, this PEDOT:PSS/Triton X-100 system has only been utilized for composite electrodes and thermoelectric application[34,36] and has not been implemented into OECTs before. Herein, we provide a report of an all solid state OECT that is self-healable and possess good electrical performance, by utilizing a matrix of PEDOT:PSS and non-ionic surfactant Triton X-100 (PEDOT:PSS/TX) as channel and ion conducting poly(vinyl alcohol) (PVA) hydrogel as a quasi-solid-state polymer electrolyte. The TX additive serves as an electrical performance booster and self-healing agent. We report for the first time that the utilization of Triton X-100 surfactant can serve to induce better morphology in PEDOT:PSS for OECT applications. We also observed physical and electrical self-healing of the PEDOT:PSS/TX film triggered by PVA hydrogel touch on the damaged area that facilitates the enhanced deformability followed by water swelling of PEDOT:PSS/TX film. Simultaneously, the PVA hydrogel modulate the PEDOT:PSS doping with high ionic conductivity around 9.8 x 10^{-3} S/cm for operating OECT device. The fabricated self-healable PEDOT:PSS/TX based OECT with PVA hydrogel electrolyte exhibits a high peak transconductance of 48 ± 5 mS (maximum 54 mS) at gate bias (V_G) of -0.1 V and on/off current ratio of ~1.5×10^3. A rise time of 6.8 ms is also attained, demonstrating the fast ion penetration in the ~2 μm thick PEDOT:PSS/TX channel. After subjecting to deliberate cut on the channel followed by healing process, the OECT showed remarkable self-healing behaviors and maintained high electrical performance with a

transconductance of ~45 mS at V_G = -0.075 V and on/off ratio of ~1.3 x 10^3. Furthermore, the healed channel shows a long-term stability even after two months of storage in ambient condition (at RH = 70%). Finally, the ion-sensing behavior of the current-driven OECTs was examined which exhibited a high ion sensitivity of 84.52 mV dec^{-1} and recovered ~95% of its ion sensitivity after healing.

RESULTS AND DISCUSSION

Here, 5.2 wt% of Triton X-100 (TX) was mixed with the PEDOT:PSS solution and utilized as an ~ 2 μm thick OECT channel through spray-deposition method. The associated fabrication process is presented in Figure S2 in the Supporting Information. First, we investigated the device performance of the spray coated PEDOT:PSS/TX film in OECT device with 0.1 M NaCl solution. Figure 1a and Figure S3 show the schematic illustration and optical image of the fabricated PEDOT:PSS/TX OECT with 0.1 M NaCl liquid electrolyte respectively. By applying a positive bias on the Ag/AgCl gate electrode, Na^+ cations move into the channel, decreasing the channel current (or drain current), owing to the reduction of $PEDOT^+$, thus initiating the de-doping process. As shown in supporting Figure S4a, the decrease in current upon the application of positive gate biasing is consistent with the depletion mode operation. Notably, the peak transconductance (g_m) of the 2 μm thick PEDOT:PSS/TX based OECT is 48.7 mS (at V_G= -0.1 V; Figure 1b). The normalized g_m (by channel geometry Wd/L) is 4.9 mS μm^{-1} which is comparable to widely reported ethylene glycol (EG)-modified PEDOT:PSS based OECTs (See Table S1).[37,38] Moreover, the device exhibits a low threshold voltage of 0.36 V and good on/off current ratio of ~2×10^4. To evaluate the effect of TX in PEDOT:PSS based OECT, spray-coated pristine PEDOT:PSS (without TX additive; similar film thickness of ~2 μm) based OECT device was compared. As shown in Figure S4b and Figure 1c, the pristine PEDOT:PSS OECT exhibited

lower drain current and maximum transconductance as 0.12 mS at V_G= -0.2 V. This result indicated that the addition of TX surfactant can serve to enhance the OECT performance. One figure-of-merit to benchmark the OECTs device performance is the product of carrier mobility (μ) and volumetric capacitance (C*), since the μC* value represents the steady-state electronic/ionic transport properties of the active materials.[39] The μC* value is extracted from equation $g_m = \frac{\partial I_D}{\partial V_G} = (Wd/L)\,\mu\, C^*\,(V_T - V_G)$ in saturation region, where the W, L and d is the channel width, length and thickness respectively, V_T is the threshold voltage, and V_G is the gate voltage. The μC* value is determined to be 91 ± 19 F cm^{-1} V^{-1} s^{-1} and is comparable to reported values from EG- and ionic liquid-modified PEDOT:PSS OECTs (Table S1).[24,37,40] We further conducted electrochemical impedance spectroscopy (EIS) measurement to determine the volumetric capacitance (C*) independently. The calculated volumetric capacitance is 38 F cm^{-3} as presented in Figure S5. Correspondingly, the channel mobility (μ) is calculated to be 2.4 ± 0.5 cm^2 V^{-1}s^{-1} (Table S1).[24,37,38,40] Moreover, the PEDOT:PSS/TX based OECT exhibited outstanding transient response of drain current at V_D= -0.5 V and square pulse of V_G= 0 to 0.6 V (pulse width= 0.5 s). From the single exponential fit, a rise time of 5.7 ms is determined, clearly indicating the fast ion penetration into the PEDOT:PSS/TX film even with the channel thickness of ~2 μm (Figure 1d). We note a relative slow recovery of the drain current which is due to slow ionic transport process.[41] The switch on behavior (OFF-to-ON) can be dramatically improved through the application of a reverse gate voltage (V_G = -0.4 V) which can assist to push the ions back to the electrolyte rapidly and improve the recovery time from 33 to 11 ms (See Figure S6 and Figure 1e). The device also maintained 97% of initial drain current value after 1000 cycles (Figure 1e) of gate pulse, which indicates the reversibility of the electrochemical processes.

These results indicate that the PEDOT:PSS/TX film is an effective channel layer for OECT operation.

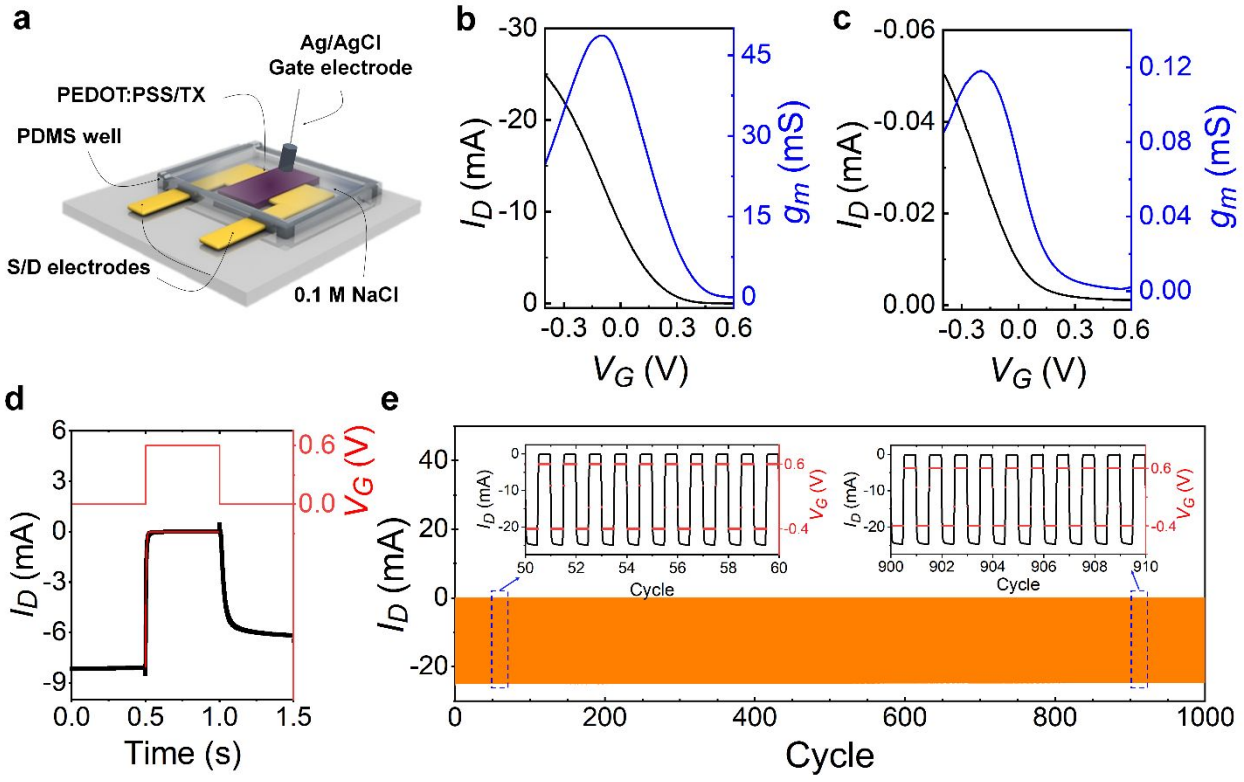

Figure 1. (a) Schematic diagram of the PEDOT:PSS/TX OECT with 0.1 M NaCl electrolyte. (b) Transfer characteristic of PEDOT:PSS/TX OECT for V_D= -0.5 V with associated transconductance (g_m). (c) Transfer characteristic of pristine PEDOT:PSS OECT for V_D= -0.5 V with associated transconductance (g_m). (d) Transient response of PEDOT:PSS/TX OECT with drain current for V_D= -0.5 V and square pulse V_G varied from 0 to 0.6 V (pulse width= 0.5 s) (red line= exponential fit with a rise time of 5.7 ms.). (e) Pulse measurement with V_G switches from -0.4 to 0.6 V for constant V_D= -0.5 V and pulse width of 0.5 s for 1000 cycling pulses in 0.1 M NaCl electrolyte.

Since the charge transport of OECT is closely related to the morphology of the channel, optical microscopy and scanning electron microscopy (SEM) were conducted to characterize the morphology of spray-coated PEDOT:PSS/TX film. The optical image of the spray-coated PEDOT:PSS/TX film in Figure 2a shows a coarser surface morphology as compared to the common coating methods such as drop casting and spin coated films (Figure S7). Such a coarser

surface morphology of spray-coated films has also been reported previously, which is due to the large droplet size during spray deposition.[42,43] From the cross-sectional SEM image, the spray-coated film also exhibited a porous and beady layered structure (Figure 2b). We speculate that the porous structure of spray-coated PEDOT:PSS/TX film promote ion penetration from the electrolyte, thereby allowing comparable electrical performance with fast response even with ~2 μm channel thickness. In addition, a low water contact angle of 33.6° of the spray-coated PEDOT:PSS/TX film endorses the good affinity for water as compared to pristine PEDOT:PSS film which exhibits a contact angle of 81.5° (See Figure 2c and 2d). We further carried out the sheet resistance measurement to look into the influence of TX on the electrical property of PEDOT:PSS. A remarkable enhancement in the electrical conductivity of the PEDOT:PSS film was observed when the content of TX increased. At ~ 5.2 wt% of TX, the measured conductivity is around 177 ± 26 S/cm (see Figure S8), which is higher than that of the pristine PEDOT:PSS film (~ 1 S/cm). Since the TX surfactant is amphiphilic, it can interact with both PEDOT and PSS, forming TX-PEDOT and TX-PSS complexes and therefore induces reorganization of the PEDOT chains and domains.[32,44] Grazing-incidence wide-angle X-ray scattering (GIWAXS) analysis was thus conducted to examine the structural changes in the PEDOT:PSS/TX film. Figure 2e and 2f compares the in-plane and out-of-plane X-ray scattering intensity of the pristine PEDOT:PSS film and PEDOT:PSS/TX film at various angles. In the case of pristine PEDOT:PSS, the distinguishing PEDOT:PSS stacking at low angle is present at 0.55 $Å^{-1}$ (d=11.36 Å) in the q_z direction corresponding to the 020 reflection[23], and the high angle scattering corresponding to PSS packing is observable as a halo at 1.25 $Å^{-1}$ in all directions, suggesting an isotropically amorphous PSS phase with a real-space distance of 5.02 Å.[45] Moreover, for the pristine film, the scattering due to π-π stacking of PEDOT is observable at

1.78 $Å^{-1}$ with a close packing distance of 3.54 Å.[38] For PEDOT:PSS/TX film, the peak at q value of around 1.41 $Å^{-1}$ was designated as the amorphous TX interaction peak. This effect is similar to previous report in EG-doped PEDOT:PSS film which observed a broad peak due to EG scattering in the initial spin-casting process.[46] After the evaporation of EG is completed, the PEDOT crystallizes and the two scattering peaks for PSS side group and PEDOT π-π stacking emerges. However, in the case of the PEDOT:PSS/TX film, the TX surfactant has a much higher boiling point of 270 °C and therefore remains in the film. We interpreted the scattering peaks by deconvoluting the scattering intensities assuming a Gaussian peak shape (Figure S9). The characteristic reflection of PEDOT π-π stacking is observed at q = 1.88 $Å^{-1}$ (3.34 Å), in good agreement with previous literature.[44] The smaller PEDOT stacking is also accompanied by an overall increase in the d-spacing for PSS side group with q = 1.06 $Å^{-1}$ (5.93 Å), hinting a possibly swollen PSS phase due to moisture uptake from ambient. Therefore, the results indicate the PEDOT:PSS/TX film features higher PEDOT connectivity and better water uptake in PSS phase, which allow both good charge transport and ion permeability for high performing OECTs.

The electrochemical doping/dedoping process of PEDOT:PSS and PEDOT:PSS/TX was further explored and compared by monitoring the change in optical absorption spectra of the films immersed in 0.1 M NaCl electrolyte under voltage bias.[22] Upon application of positive voltages and therefore injection of Na^+ cations, the pristine PEDOT:PSS film switched from oxidized to neutral state, as evidenced by the appearance of a band at 645 nm due to the π-π* transition of neutral PEDOT (Figure 2g). Under zero bias, PEDOT film is highly conducting with high carrier concentration, due to the presence of mostly bipolaronic charge carriers, as established by the absorption band above 970 nm.[47,48] With the increase in voltage bias to 0.5 V, the population of mostly bipolaronic PEDOT shifts to a combination of mostly polaronic

PEDOT (600-900 nm), and neutral PEDOT (400-600 nm). Finally, at 1 V, the PEDOT is almost completely switched to its neutral semiconducting state, evidenced by the predominant absorption band in the visible region. In the case of PEDOT:PSS/TX film, however, it showed a relatively higher absorption band above 970 nm, suggesting a higher doping level than the pristine PEDOT film (Figure 2h).[22]

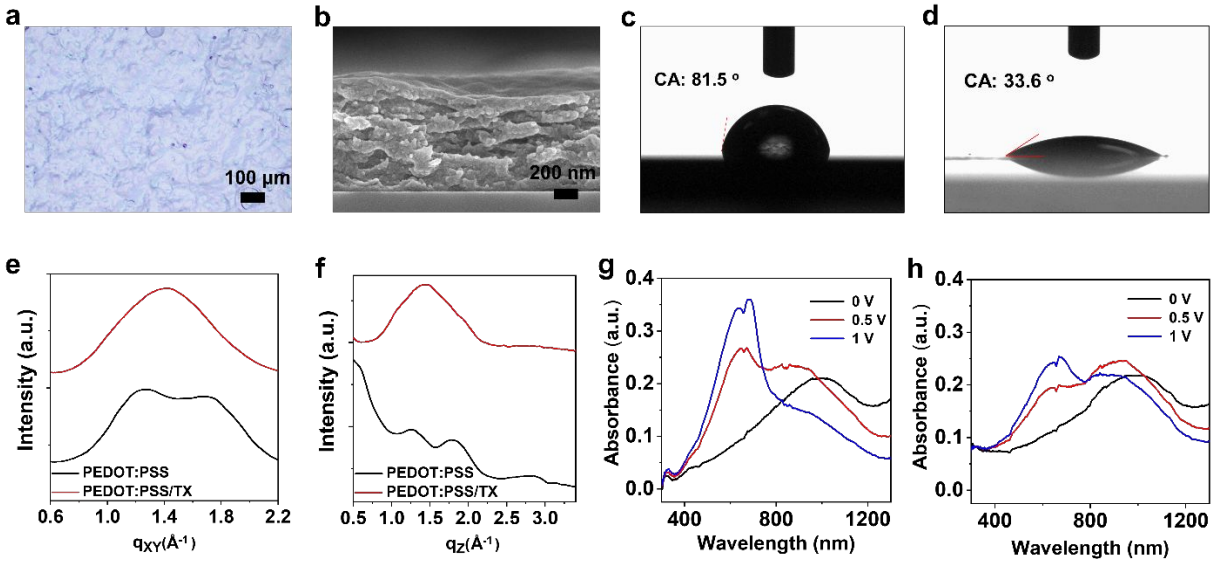

Figure 2. (a) Top-view optical microscopy image of spray coated PEDOT:PSS/TX film (Scale bar: 100 µm). (b) Cross-sectional Scanning Electron Microscopy (SEM) image of spray coated PEDOT:PSS/TX film (Scale bar: 200 nm). Water contact angle (CA) of spray coated (c) pristine PEDOT:PSS film and (d) PEDOT:PSS/TX film. (e) In plane and (f) out of plane GIWAXS of pristine PEDOT:PSS film and PEDOT:PSS/TX film on SiO_2 wafer. UV-vis-NIR spectroelectrochemical data from 0 to 1 V for (g) pristine PEDOT:PSS film and (h) PEDOT:PSS/TX film in 0.1 M NaCl electrolyte.

The PEDOT:PSS/TX based OECT also revealed comparable electrical performance when using Na^+ ion conducting PVA hydrogel as a quasi-solid-state electrolyte (Figure 3a). The PVA hydrogel acts as electrolyte connecting the gate to the channel and was prepared by freeze-thaw method.[49] The transparent PVA hydrogel was chosen as it exhibits good mechanical properties, good biocompatibility and high-water content. In addition, when soaked in salt solution, the PVA hydrogel is found to have enhanced mechanical strength due to the increase in hydrophobic

interchain interaction.[50] The strong adhesion property of PVA hydrogel gives rise to sufficient contact with PEDOT:PSS/TX layer thereby enabling efficient ion penetration and transport into the active channel layer. The PVA hydrogel showed a high swelling ratio of 114 ± 2.82 % after immersing in DI water for 24 hours. In this work, sodium ions were added into the PVA hydrogel which serve to modulate the doping and dedoping process in the channel of OECT with a high ionic conductivity of around 9.8 x 10^{-3} S/cm (Figure S10). As shown in Figure 3b-c, the PEDOT:PSS/TX based OECT with PVA hydrogel electrolyte exhibits high transconductance of 48 ± 5 mS (maximum 54 mS) at V_G= -0.1 V and on/off current ratio of ~1.5×10^3 which is comparable with the result with liquid electrolyte. Moreover, the transient response of drain current shows a rise time of 6.8 ms and maintaining 98% of drain current after 1000 cycles (Figure S11). Therefore, by utilizing the ion conductive PVA hydrogel as an electrolyte, the OECT channel can function stably with good electrical performance.

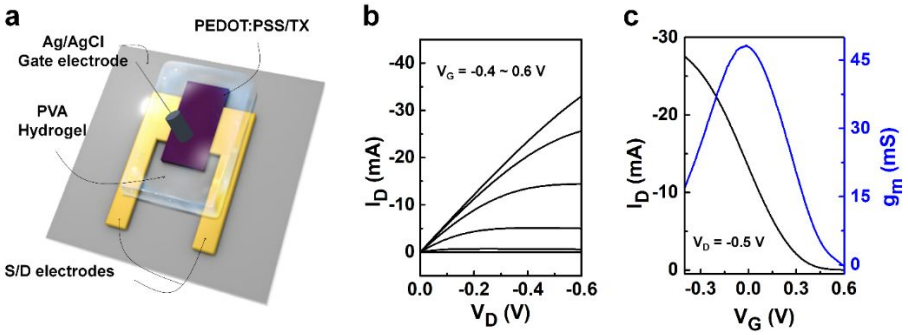

Figure 3. (a) Schematic diagram of the PEDOT:PSS/TX OECT with hydrogel which is swelled in 0.1 M NaCl electrolyte. (b) Output characteristic for V_G= -0.4 V (top curve) to 0.6 V (bottom curve) (step: 0.2 V). (c) Transfer characteristic for V_D= -0.5 V with associated transconductance (g_m).

To evaluate the self-healability, a PEDOT:PSS/TX film (~2 μm thick) was prepared on the PDMS substrate. After that, the PDMS substrate was stretched ~30% and released to generate small cracks on PEDOT:PSS/TX film. To minimize the damages on Au electrodes, we used pre-

stretched PDMS substrate for Au electrode evaporation and released it before spray coating the PEDOT:PSS/TX film (Figure S12). Figure 4a-b show a schematic illustration and corresponding microscope image of the PEDOT:PSS/TX film before and after healing. As shown in Figure 4a-b, the damaged area was healed after putting the PVA hydrogel (swelled in 0.1 M NaCl solution) on the film. The electrical healing of the PEDOT:PSS/TX film was also demonstrated by measuring the current values during the self-healing test as shown in Figure 4c. Clearly, the current level was recovered to almost 100% of the initial value upon placing the PVA hydrogel on the damaged area. Therefore, we investigated the OECT performance of the PEDOT:PSS/TX film on the PDMS substrate after healing the film from the strain stress. As shown in Figure 4d and e, the OECT device which is fabricated on PDMS substrate exhibited a good electrical self-healability before and after self-healing from the damages which are induced by stretching the PEDOT:PSS/TX films. From the transfer curve, the healed PEDOT:PSS/TX OECT showed drain current of 6.48 mA which is recovered to 95% of initial drain current from fresh channel (6.79 mA). Moreover, the transconductance was recovered to 99.6% (16.40 mS) of its initial value (16.46 mS) thereby indicating the outstanding electrical self-healing characteristic. To the best of our knowledge, this is the first demonstration of an OECT channel with quasi-solid-state electrolyte to possess simultaneous good electronic/ionic transport and >95% recovery in electrical performance after mechanical damage. In addition, we expect that the stretchability and electromechanical property of PEDOT:PSS/TX OECT can be further improved by incorporating plasticizer such as low molecular weight polyethylene glycol.[51]

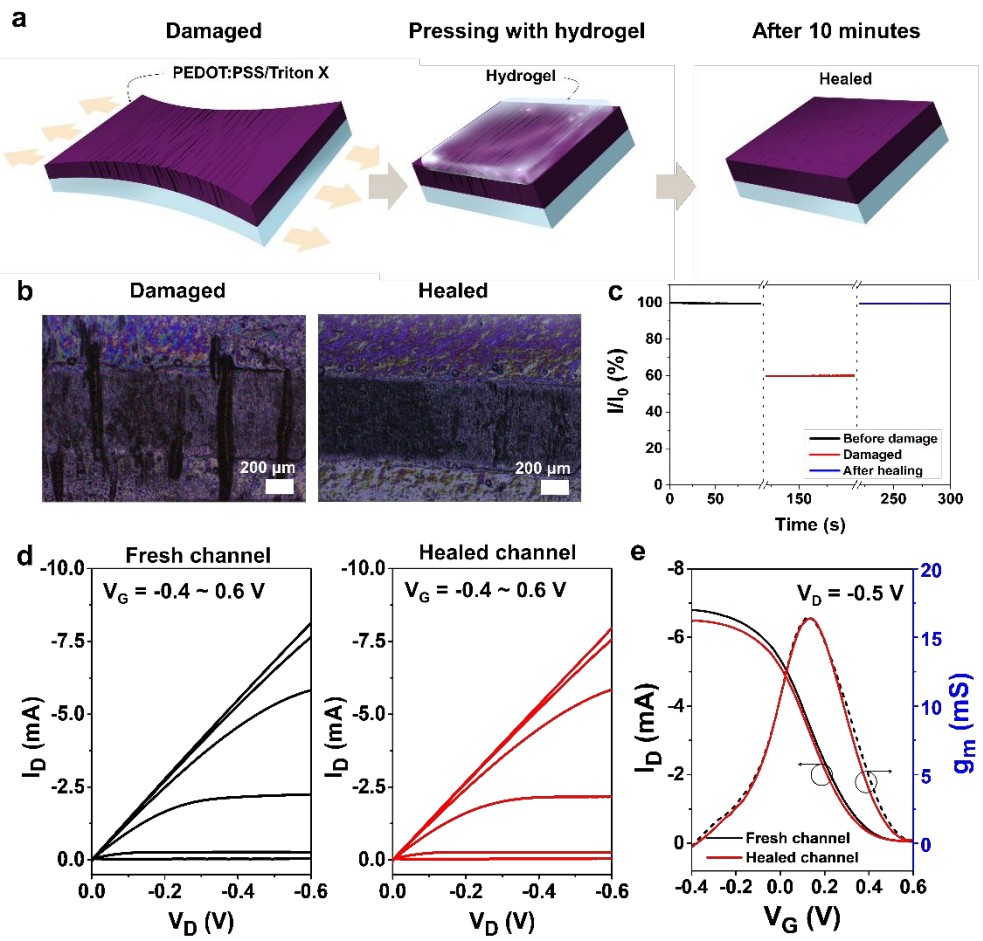

Figure 4. (a) Schematic illustration of the PEDOT:PSS/TX self-healable polymer matrix with the PVA hydrogel on top. (b) Optical microscope images of PEDOT:PSS/TX film before and after the self-healing process (Scale bar: 200 μm). (c) Current change of PEDOT:PSS/TX film during the self-healing test. (d) Output characteristic of PEDOT:PSS/TX OECT on PDMS substrate of before and after self-healing for V_G= -0.4 (top curve) to 0.6 V (bottom curve) (step: 0.2 V). (e) Transfer characteristic of before and after self-healing for V_D= -0.5 V with associated transconductance (g_m).

Repair of damages on the polymer film can be in general described in terms of following process: (a) surface rearrangement, (b) surface approach, (c) wetting, (d) diffusion, and (e) randomization of polymer.[52] The healing process in PEDOT:PSS/TX system has been attributed to the plasticizing and viscoelastic effect of the TX surfactant, where the motion of the polymer chains are enhanced to move across the damaged area facilitated by pressure contact.[34] The

pressure contact can be in the form of any physical touch. In other words, the damaged area can be healed as long as they were joined together under proper pressure contact. However, we note that the PEDOT:PSS/TX film with poly(dimethyl siloxane) (PDMS) block for contact does not have good healing properties (Figure S13) and the current recovery is ~42% (Figure S14 and Video S2). This is most likely due to the thinner film thickness employed (~1 to 2 μm thick) where the surface rearrangement is lower as compared to previous report which uses a thick dough (~50 μm).[34] In contrast to PDMS, the PVA hydrogel exhibits great ion conductivity and also serves as solid electrolyte for OECTs. Upon contact with PVA hydrogel, the damaged area was swelled owing to the water uptake by PSS^- chains, leading to enhanced deformability and softness of the PEDOT:PSS/TX film and thus further aiding in the repair of the cracks on the polymer films.[33]

To further evaluate the water healing effect, nano-cracks were generated by overstretching the PEDOT:PSS/TX film and these damaged areas were exposed to water vapor alone. As can be seen in Figure S15, the cracks were immediately healed. It is therefore possible to heal the system with water, especially if the damage area is not severe. Therefore, the swelling of the PEDOT:PSS/TX film assists surface rearrangement of damaged area to repair the cracks on the polymer films. However, where we deliberately cut the whole film (~1 μm thick) with a razor blade, the healing of these enlarged damaged area is not effective using water vapor only and we could obtain the current recovery rate more than 80% of initial values by healing the damaged area with both physical contact and water (i.e. using PVA hydrogel); Figure S16 and Video S1, Supporting Information). Therefore, the synergistic effect of physical deformation and water swelling of PEDOT:PSS/TX channel from the PVA hydrogel electrolyte plays an important role in accelerating the self-healability.

We further investigate the self-healing performance of PEDOT:PSS/TX OECT which is fabricated on silicon dioxide substrate after subjecting the whole channel to razor blade cut followed by healing process. In this study, we first removed the PVA hydrogel from the channel layer after the initial device characterization and deliberately cut the center of the whole channel with a razor blade to test the device with a more fatal damage (Figure 5a, the device structure is shown in Figure 3a and Figure S3c-d). Next, the PVA hydrogel was placed onto the damaged channel layer and allowed it to heal for 10 minutes. As shown in the SEM characterization in Figure 5a, the damaged channel area was recovered. Coincidently, the drain current of the OECT recovered to 85% of its initial value and the transconductance was recovered to 84% (45.3 mS) of the initial value (54 mS) (Figure 5c). Moreover, the healed device showed high switching stability, where the drain current retained 86 % of the original value after 1000 cycles (Figure S17, Supporting Information). The stability of healed devices was also investigated (Figure 5c). Remarkably, after 68 days of storage under ambient condition (RH = 70%), the drain current was found to increase and recovered to 95% of initial value while the transconductance recovered to 47 mS (87% of initial value). The enhanced electrical properties over time indicate that the PEDOT:PSS/TX channel layer continue to heal in the ambient condition due to the viscoelastic polymer chain movement in PEDOT:PSS/TX matrix.[34,53,54] Additionally, we recorded the current changes during several cut-and-healing processes to verify the reusability of this self-healable PEDOT:PSS/TX film (~ 2 μm). It was observed that the current immediately returned to its highly conducting state when the PVA hydrogel was gently touched the damage area. Over 80% of the initial current was maintained after five times of cut-and-healing processes (Figure S18).

Finally, we investigate the ion sensing capability of the self-healable PEDOT:PSS/TX OECTs to demonstrate their potential for future wearable bioelectronic applications. In particular,

OECTs are receiving substantial attention for ion sensing applications due to their high sensitivity and low operating voltages which are essential for biological and chemical detection in aqueous media. Here, we utilized the PEDOT:PSS/TX OECT to detect the Na^+ ions in the PVA hydrogel which are swelled in different concentration of salt solutions. We investigate the voltage ion sensitivity in a current driven OECT configuration (Figure 5d). Such a circuit configuration has been shown to enhance the ion sensitivity.[22,55] The input voltage V_I is applied to the gate, and the output voltage V_O is characterized while a bias current I_D is set by the current source. Figure S19a shows the transfer characteristic ($V_O - V_I$) by varying I_D from -350 μA to -1.1 mA with a step of -250 μA. While applying positive voltages at V_I, Na^+ cations are injected to the PEDOT:PSS/TX channel layer and the channel layer is de-doped, eventually the PEDOT:PSS/TX OECT is operated in saturation region. Thus, the distinct transition between the linear and the saturation region take place at the pinch-off voltage. As shown in Figure S19b, by increasing the ion concentration from 0.01 to 1 M, the minimum V_I (V_{SW}) to switch the transistor from linear to saturation region is decreased from 0.49 to 0.325 V under I_D= -1.1 mA. The ion sensitivity of the current-driven PEDOT:PSS/TX OECTs was investigated by calculating the cumulative shift of the V_{SW} under I_D= -1.1 mA, defined as $\Delta V_{SWi+1} = \Delta V_{SWi} + (V_{SWi+1} - V_{SWi})$. The PEDOT:PSS/TX OECT exhibited a high ion sensitivity of 84.52 mV dec^{-1} (Figure 5e), which is higher than the theoretical Nernstian sensitivity of 59.2 mV dec^{-1}. Interestingly, the ion sensing characteristics of PEDOT:PSS/TX OECT after the cut-and-heal test remained almost unchanged. The healed device showed similar transfer characteristics as the fresh device (Figure S19c-d, Supporting Information) and the ion sensitivity of healed device was 80.5 mV dec^{-1} which is recovered to 95% of the original value (Figure 5f). Therefore, the PEDOT:PSS/TX has

great potential as a self-healable OECT channel to effectively detect ions in wearable biosensors and healthcare applications.

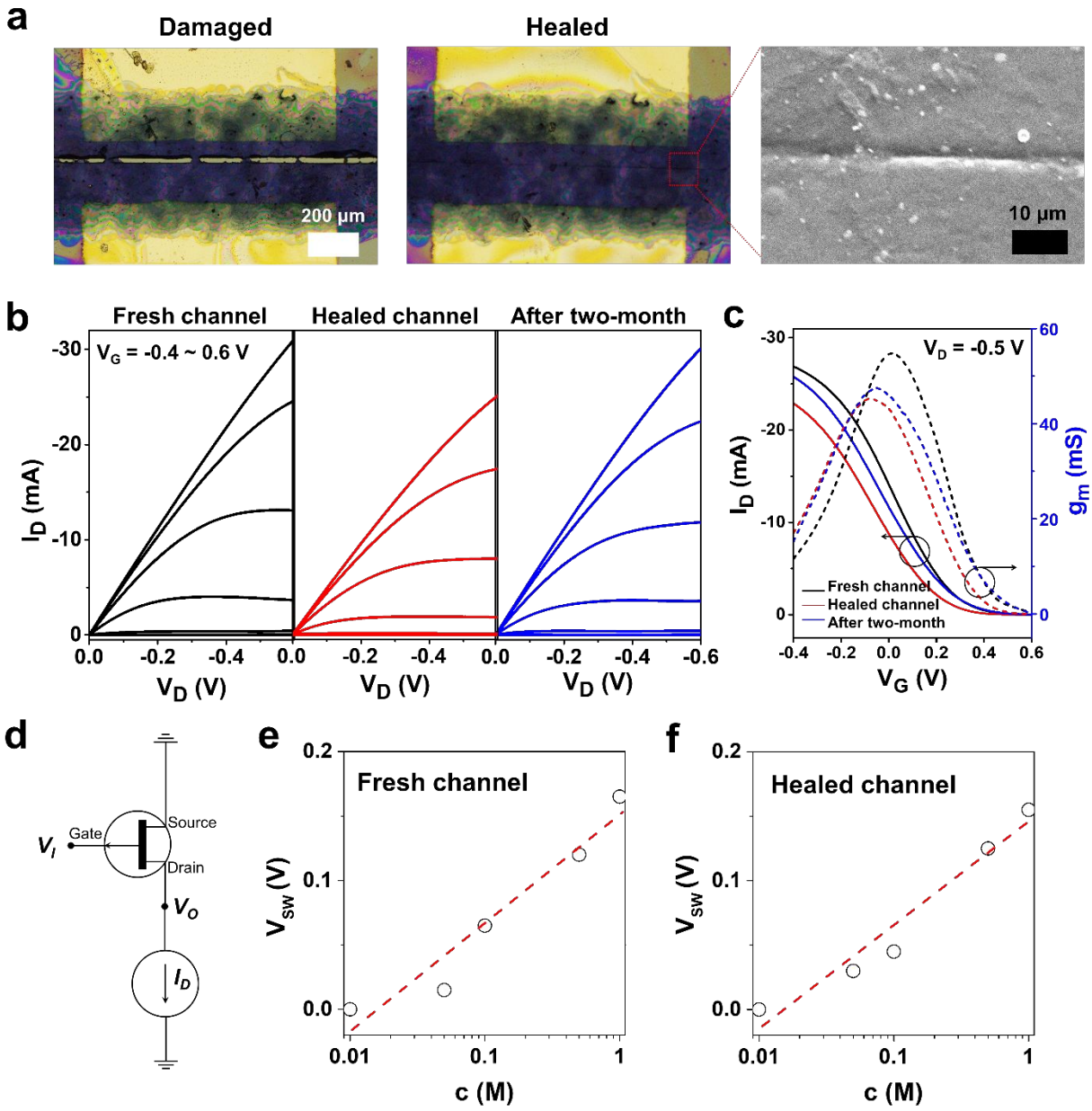

Figure 5. (a) Optical images of damaged and healed PEDOT:PSS/TX channel layer (Scale bar: 200 μm) and enlarged SEM image of healed area (Scale bar: 10 μm). (b) Output characteristic of PEDOT:PSS/TX OECT on silicon dioxide substrate of before and after self-healing for V_G= -0.4 V (top curve) to 0.6 V (bottom curve) (step: 0.2 V). (c) Transfer characteristic of before and after self-healing for V_D= -0.5 V with associated transconductance (g_m). (d) Configuration of a current

driven OECT. Cumulative switching voltage variation of PEDOT:PSS/TX OECT versus ion concentration (e) before damage and (f) after healing.

CONCLUSIONS

In summary, we have developed a self-healable and high performing OECT using PEDOT:PSS/TX channel and PVA hydrogel electrolyte. The physical and electrical self-healing of the PEDOT:PSS/TX film was triggered by PVA hydrogel touch on the damaged area and self-healability was observable even at a thickness as low as 1 μm. PEDOT:PSS/TX film also features higher PEDOT connectivity and better water uptake in PSS phase, which allow both good charge transport and ion permeability for high performing OECTs. Therefore, the PEDOT:PSS/TX OECT with PVA hydrogel electrolyte exhibits a high peak transconductance of 48 ± 5 mS (maximum 54 mS), on/off current ratio of ~1.5×10^3, fast response time of 6.8 ms and high switching stability (maintained ~98% of drain current after 1000 cycles. Simultaneously, the OECT showed good self-healing behaviors after mechanical damage and maintained high electrical performance with a transconductance of ~45 mS at V_G = -0.075 V and on/off ratio of ~1.3 x 10^3. Moreover, the healed device showed good operational stability after 68 days of storage in ambient condition. We also report the ion-sensing behavior of the current-driven OECTs which exhibited a high ion sensitivity of 84.52 mV dec^{-1} and recover ~95% of its ion sensitivity after healing. The presented work will open up a new vista for developing smart devices that would strike a balance providing high electrical performance, high ion sensitivity while also demonstrating self-healing and would find great applications in most wearable bioelectronic systems, increasing the durability and reliability.

EXPERIMENTAL SECTION

Materials: poly(3,4-ethylenedioxythiophene):poly(styrenesulfonate) (PEDOT:PSS) (Clevios PH1000) was obtained from Heraeus. Triton X-100, sodium chloride (NaCl), (3-glycidoxypropyl)trimethoxysilane (GOPS) and poly(vinyl alcohol) (PVA) (99% hydrolyzed, MW 146-186k) were purchased from Sigma-Aldrich. Poly(dimethyl siloxane) (PDMS) (Sylgard 184) was purchased from Dow Corning Corp.

Film preparation: The PEDOT:PSS/TX solution was prepared by mixing 52 mg non-ionic surfactant Triton X-100 and 1g aqueous PEDOT:PSS (1.3 wt%) with 1 wt% of 3-glycidyloxypropyl)trimethoxysilane (GOPS), and stirred vigorously for 30 min. In this work, GOPS was added into the mixture of PEDOT:PSS/TX solution for increasing the stability under the aqueous environment. The PVA hydrogel was prepared by dissolving 16 wt% of PVA in DI water at 95 ^{o}C. For gelation of PVA solution, the solution was casted on the glass petri dish and kept in the freeze for 3hrs and thawed 18hrs in ambient condition. The prepared gel was cut to the required size by razor blade and swelled in DI water or 0.1 M NaCl solution for 24hrs before use. The swelling ratio of hydrogel was calculated by following equation: swelling ratio (%) = (WS-WD)*100/WS; where WS is weight of the PVA hydrogel after soaking in solution and WD is weight of the PVA hydrogel before soaking in solution.

Device fabrication: To fabricate OECT devices, silicon wafers with 200 nm thermal grown SiO_2 were used as a substrate. The substrate was cleaned with acetone and isopropyl alcohol and dried with nitrogen. The cleaned substrate was exposed to ultraviolet ozone (UVO) for 30min. The 100 nm thick of gold source/drain electrodes were deposited on the cleaned substrate by thermal evaporation (W/L: 1000/200 μm). To protect the gold contact electrodes, PMMA patterns were prepared as reported in the previous literatures.[22,56] After removing PMMA layer on the channel area, the active channel layer was patterned by spray-coating PEDOT:PSS/TX solution through a

stencil mask using a commercial airbrush unit (Model ASG-Ko82; flow rate: 2 ml min^{-1}) on the hotplate at 140 ^{o}C.[24] Subsequently, PDMS well or hydrogel was introduced on the top of the channel layer for characterization (see Figure S3, Supporting information). Photographs and cross-sectional images of tested PEDOT:PSS/TX OECT devices are shown in Figure S3, Supporting information. A total of 10 devices were prepared and tested. To fabricate the OECT on PDMS substrate, 500 μm thick PDMS mold was prepared by curing PDMS at 60 ^{o}C for 6 hrs. On the ~30% stretched PDMS substrate, the 100 nm thick gold source/drain electrodes were deposited. After releasing the gold deposited PDMS substrate, PEDOT:PSS/TX layer was spray-coated through a stencil mask with same procedure as mentioned above.

Characterization: To demonstrate self-healing test, Leica 818 blade (0.35mm thick) was used. Top-view images of before and after healed PEDOT:PSS/TX films were investigated by scanning electron microscopy (SEM) (JSM-7600F, JEOL). Electrochemical Impedance Spectrum (EIS) was employed to extract the ionic conductivity of the PVA hydrogel using potentiostat/galvanostat instrument (PGSTAT 128N, Autolab). In brief, the PVA hydrogel sample was assembled in a coin cell sandwiched between two stainless steels. The ionic conductivity (σ) of the hydrogel was extracted from the equation of $\sigma = {}^{d}/_{R_s A}$, where d is the hydrogel thickness, R_s is the electrolyte resistance, and A is the cross-sectional area of the sample. The EIS was also performed to extract the volumetric capacitance of the PEDOT:PSS/TX film using a three-terminal configuration, in which the PEDOT:PSS film was deposited on top of Ni/Au electrode and used as the working electrode, with a standard Ag/AgCl wire and Pt mesh as reference electrode and counter electrode, respectively. The measurement was operated in 0.1 M NaCl solution. Water contact angle was measured by optical contact angle measurement system (OCA 15EC, DataPhysics). Molecular packing of PEDOT:PSS and PEDOT:PSS/TX

layer were studied by grazing incidence wide angle X-ray diffraction (GIWAXS) (Nanoinxider, Xenocs). Absorption spectra of the polymer films were recorded on UV-VIS spectrophotometer (UV-3600, Shimadzu). The crystallinity of the films was identified using XRD (D8 Advance, Bruker). Thickness of the polymer films were characterized with Alpha-Step profilemeter (KLA-Tencor). The I-V characteristic of the films, and all the OECT device characteristics including output and transfer curve and pulse measurement were measured under ambient condition using Keysight precision source/measure unit (B2912A).

Supporting Information

Supporting Information is available from the Wiley Online Library or from the author. Molecular structure of PEDOT:PSS and Triton X-100; schematic illustration of device fabrication procedure; photograph and cross-sectional schematic of PEDOT:PSS/TX OECT; output curves of the PEDOT:PSS/TX and pristine PEDOT:PSS OECT; top-view optical microscopy image and cross-sectional scanning electron microscopy (SEM) image of drop-cast PEDOT:PSS/TX film; electrical conductivity of the PEDOT:PSS/TX film; Optical images of the PVA hydrogel with associated swelling properties, Electrochemical Impedance Spectra (EIS) of spray-deposited PEDOT:PSS/TX film and PVA hydrogel in 0.1 M NaCl solution; Comparison of the transconductance and threshold voltage (V_t) of PEDOT:PSS-based OECTs; transient response of the PEDOT:PSS/TX OECT with PVA as electrolyte, and the associated stability study; Out of plane GIWAXS of PEDOT:PSS/TX film on SiO_2 wafer with the deconvoluted curves; schematic illustration of the self-healing process for PEDOT:PSS/TX OECT on PDMS substrate; optical images of damaged film healed with PDMS; electrical recovery of the PEDOT:PSS/TX film healed by PDMS; water vapor assisted to heal the nano-cracks of PEDOT:PSS/TX film; electrical recovery of a damaged PEDOT:PSS/TX film healed with PVA hydrogel; the electrical performance of a current-driven PEDOT:PSS/TX OECT before and after healing.

Acknowledgements

W. L. Leong would like to acknowledge funding support from her NTU start-up grant (M4081866), Ministry of Education (MOE) under AcRF Tier 2 grant (2018-T2-1-075) and A*STAR AME Young Individual Research Grant (Project Number A1784c019). We would like to acknowledge the Facility for Analysis, Characterization, Testing and Simulation (FACTS), Nanyang Technological University, Singapore, for use of their GIWAXS facility (Xenocs Nano-inXider).

References

(1) Kayser, L. V; Lipomi, D. J. Stretchable Conductive Polymers and Composites Based on PEDOT and PEDOT:PSS. *Adv. Mater.* **2019**, *31*, 1806133.

(2) Facchetti, A. π-Conjugated Polymers for Organic Electronics and Photovoltaic Cell Applications †. *Chem. Mater.* **2011**, *23*, 733–758.

(3) Khodagholy, D.; Doublet, T.; Gurfinkel, M.; Quilichini, P.; Ismailova, E.; Leleux, P.; Herve, T.; Sanaur, S.; Bernard, C.; Malliaras, G. G. Highly Conformable Conducting Polymer Electrodes for In Vivo Recordings. *Adv. Mater.* **2011**, *23*, H268–H272.

(4) Liao, C.; Zhang, M.; Yao, M. Y.; Hua, T.; Li, L.; Yan, F. Flexible Organic Electronics in Biology: Materials and Devices. *Adv. Mater.* **2015**, *27*, 7493–7527.

(5) Bendrea, A.-D.; Cianga, L.; Cianga, I. Review Paper: Progress in the Field of Conducting Polymers for Tissue Engineering Applications. *J. Biomater. Appl.* **2011**, *26*, 3–84.

(6) Tybrandt, K.; Zozoulenko, I. V; Berggren, M. Chemical Potential–Electric Double Layer Coupling in Conjugated Polymer–Polyelectrolyte Blends. *Sci. Adv.* **2017**, *3*, eaao3659.

(7) Lin, P.; Yan, F.; Chan, H. L. W. W. Ion-Sensitive Properties of Organic Electrochemical Transistors. *ACS Appl. Mater. Interfaces.* **2010**, *2*, 1637–1641.

(8) Kim, Y.; Lim, T.; Kim, C.-H.; Yeo, C. S.; Seo, K.; Kim, S.-M.; Kim, J.; Park, S. Y.; Ju, S.; Yoon, M.-H. Organic Electrochemical Transistor-Based Channel Dimension-Independent Single-Strand Wearable Sweat Sensors. *NPG Asia Mater.* **2018**, *10*, 1086–1095.

(9) Tang, H.; Yan, F.; Lin, P.; Xu, J.; Chan, H. L. W. Highly Sensitive Glucose Biosensors Based on Organic Electrochemical Transistors Using Platinum Gate Electrodes Modified with Enzyme and Nanomaterials. *Adv. Funct. Mater.* **2011**, *21*, 2264–2272.

(10) Kergoat, L.; Piro, B.; Simon, D. T.; Pham, M.-C.; Noël, V.; Berggren, M. Detection of Glutamate and Acetylcholine with Organic Electrochemical Transistors Based on Conducting Polymer/Platinum Nanoparticle Composites. *Adv. Mater.* **2014**, *26*, 5658–5664.

(11) Bihar, E.; Deng, Y.; Miyake, T.; Saadaoui, M.; Malliaras, G. G.; Rolandi, M. A Disposable Paper Breathalyzer with an Alcohol Sensing Organic Electrochemical

Transistor. *Sci. Rep.* **2016**, *6*, 27582.

(12) Tao, W.; Lin, P.; Hu, J.; Ke, S.; Song, J.; Zeng, X. A Sensitive DNA Sensor Based on an Organic Electrochemical Transistor Using a Peptide Nucleic Acid-Modified Nanoporous Gold Gate Electrode. *RSC Adv.* **2017**, *7*, 52118–52124.

(13) Lin, P.; Luo, X.; Hsing, I. M.; Yan, F. Organic Electrochemical Transistors Integrated in Flexible Microfluidic Systems and Used for Label-Free DNA Sensing. *Adv. Mater.* **2011**, *23*, 4035–4040.

(14) Lin, P.; Yan, F.; Yu, J.; Chan, H. L. W.; Yang, M. The Application of Organic Electrochemical Transistors in Cell-Based Biosensors. *Adv. Mater.* **2010**, *22*, 3655–3660.

(15) Rivnay, J.; Ramuz, M.; Leleux, P.; Hama, A.; Huerta, M.; Owens, R. M. Organic Electrochemical Transistors for Cell-Based Impedance Sensing. *Appl. Phys. Lett.* **2015**, *106*, 043301.

(16) Chen, L.; Fu, Y.; Wang, N.; Yang, A.; Li, Y.; Wu, J.; Ju, H.; Yan, F. Organic Electrochemical Transistors for the Detection of Cell Surface Glycans. *ACS Appl. Mater. Interfaces.* **2018**, *10*, 18470–18477.

(17) Nilsson, D.; Chen, M.; Kugler, T.; Remonen, T.; Armgarth, M.; Berggren, M. Bi-Stable and Dynamic Current Modulation in Electrochemical Organic Transistors. *Adv. Mater.* **2002**, *14*, 51–54.

(18) Zeglio, E.; Inganäs, O. Active Materials for Organic Electrochemical Transistors. *Adv. Mater.* **2018**, *30*, 1800941.

(19) Rivnay, J.; Inal, S.; Collins, B. A.; Sessolo, M.; Stavrinidou, E.; Strakosas, X.; Tassone, C.; Delongchamp, D. M.; Malliaras, G. G. Structural Control of Mixed Ionic and Electronic Transport in Conducting Polymers. *Nat. Commun.* **2016**, *7*, 11287.

(20) Giridharagopal, R.; Flagg, L. Q.; Harrison, J. S.; Ziffer, M. E.; Onorato, J.; Luscombe, C. K.; Ginger, D. S. Electrochemical Strain Microscopy Probes Morphology-Induced Variations in Ion Uptake and Performance in Organic Electrochemical Transistors. *Nat. Mater.* **2017**, *16*, 737–742.

(21) Giovannitti, A.; Sbircea, D.-T.; Inal, S.; Nielsen, C. B.; Bandiello, E.; Hanifi, D. A.;

Sessolo, M.; Malliaras, G. G.; McCulloch, I.; Rivnay, J. Controlling the Mode of Operation of Organic Transistors through Side-Chain Engineering. *Proc. Natl. Acad. Sci.* **2016**, *113*, 12017–12022.

(22) Wu, X.; Surendran, A.; Ko, J.; Filonik, O.; Herzig, E. M.; Müller-Buschbaum, P.; Leong, W. L. Ionic-Liquid Doping Enables High Transconductance, Fast Response Time, and High Ion Sensitivity in Organic Electrochemical Transistors. *Adv. Mater.* **2019**, *31*, 1805544.

(23) Kee, S.; Kim, N.; Kim, B. S.; Park, S.; Jang, Y. H.; Lee, S. H.; Kim, J. J.; Kim, J. J.; Kwon, S.; Lee, K. Controlling Molecular Ordering in Aqueous Conducting Polymers Using Ionic Liquids. *Adv. Mater.* **2016**, *28*, 8625–8631.

(24) Wu, X.; Surendran, A.; Moser, M.; Chen, S.; Muhammad, B. T.; Maria, I. P.; McCulloch, I.; Leong, W. L. Universal Spray-Deposition Process for Scalable, High-Performance, and Stable Organic Electrochemical Transistors. *ACS Appl. Mater. Interfaces.* **2020**, *12*, 20757–20764.

(25) Wang, Y.; Zhu, C.; Pfattner, R.; Yan, H.; Jin, L.; Chen, S.; Molina-Lopez, F.; Lissel, F.; Liu, J.; Rabiah, N. I.; Chen, Z.; Chung, J. W.; Linder, C.; Toney, M. F.; Murmann, B.; Bao, Z. A Highly Stretchable, Transparent, and Conductive Polymer. *Sci. Adv.* **2017**, *3*, e1602076.

(26) Gualandi, I.; Marzocchi, M.; Achilli, A.; Cavedale, D.; Bonfiglio, A.; Fraboni, B. Textile Organic Electrochemical Transistors as a Platform for Wearable Biosensors. *Sci. Rep.* **2016**, *6*, 33637.

(27) Parlak, O.; Keene, S. T.; Marais, A.; Curto, V. F.; Salleo, A. Molecularly Selective Nanoporous Membrane-Based Wearable Organic Electrochemical Device for Noninvasive Cortisol Sensing. *Sci. Adv.* **2018**, *4*, eaar2904.

(28) Campana, A.; Cramer, T.; Simon, D. T.; Berggren, M.; Biscarini, F. Electrocardiographic Recording with Conformable Organic Electrochemical Transistor Fabricated on Resorbable Bioscaffold. *Adv. Mater.* **2014**, *26*, 3874–3878.

(29) Lang, U.; Naujoks, N.; Dual, J. Mechanical Characterization of PEDOT:PSS Thin Films. *Synth. Met.* **2009**, *159*, 473–479.

(30) Noh, J.-S. Highly Conductive and Stretchable Poly(Dimethylsiloxane):Poly(3,4-Ethylenedioxythiophene):Poly(Styrene Sulfonic Acid) Blends for Organic Interconnects. *RSC Adv.* **2014**, *4*, 1857–1863.

(31) Vosgueritchian, M.; Lipomi, D. J.; Bao, Z. Highly Conductive and Transparent PEDOT:PSS Films with a Fluorosurfactant for Stretchable and Flexible Transparent Electrodes. *Adv. Funct. Mater.* **2012**, *22*, 421–428.

(32) Oh, J. Y.; Shin, M.; Lee, J. B.; Ahn, J.-H.; Baik, H. K.; Jeong, U. Effect of PEDOT Nanofibril Networks on the Conductivity, Flexibility, and Coatability of PEDOT:PSS Films. *ACS Appl. Mater. Interfaces.* **2014**, *6*, 6954–6961.

(33) Zhang, S.; Cicoira, F. Water-Enabled Healing of Conducting Polymer Films. *Adv. Mater.* **2017**, *29*, 1–6.

(34) Oh, J. Y.; Kim, S.; Baik, H.-K.; Jeong, U. Conducting Polymer Dough for Deformable Electronics. *Adv. Mater.* **2016**, *28*, 4455–4461.

(35) Kee, S.; Haque, M. A.; Corzo, D.; Alshareef, H. N.; Baran, D. Self-Healing and Stretchable 3D-Printed Organic Thermoelectrics. *Adv. Funct. Mater.* **2019**, *29*, 1905426.

(36) Zhang, S.; Chen, Y.; Liu, H.; Wang, Z.; Ling, H.; Wang, C.; Ni, J.; Çelebi-Saltik, B.; Wang, X.; Meng, X.; Kim, H.; Baidya, A.; Ahadian, S.; Ashammakhi, N.; Dokmeci, M. R.; Travas-Sejdic, J.; Khademhosseini, A. Room-Temperature-Formed PEDOT:PSS Hydrogels Enable Injectable, Soft, and Healable Organic Bioelectronics. *Adv. Mater.* **2020**, *32*, 1904752.

(37) Khodagholy, D.; Rivnay, J.; Sessolo, M.; Gurfinkel, M.; Leleux, P.; Jimison, L. H.; Stavrinidou, E.; Herve, T.; Sanaur, S.; Owens, R. M.; Malliaras, G. G. High Transconductance Organic Electrochemical Transistors. *Nat. Commun.* **2013**, *4*, 2133.

(38) Kim, S.-M.; Kim, C.-H.; Kim, Y.; Kim, N.; Lee, W.-J.; Lee, E.-H.; Kim, D.; Park, S.; Lee, K.; Rivnay, J.; Yoon, M.-H. Influence of PEDOT:PSS Crystallinity and Composition on Electrochemical Transistor Performance and Long-Term Stability. *Nat. Commun.* **2018**, *9*, 3858.

(39) Inal, S.; Malliaras, G. G.; Rivnay, J. Benchmarking Organic Mixed Conductors for Transistors. *Nat. Commun.* **2017**, *8*, 1767.

(40) Rivnay, J.; Leleux, P.; Ferro, M.; Sessolo, M.; Williamson, A.; Koutsouras, D. A.; Khodagholy, D.; Ramuz, M.; Strakosas, X.; Owens, R. M.; Benar, C.; Badier, J.-M.; Bernard, C.; Malliaras, G. G. High-Performance Transistors for Bioelectronics through Tuning of Channel Thickness. *Sci. Adv.* **2015**, *1*, e1400251.

(41) Andersson Ersman, P.; Nilsson, D.; Kawahara, J.; Gustafsson, G.; Berggren, M. Fast-Switching All-Printed Organic Electrochemical Transistors. *Org. Electron.* **2013**, *14*, 1276–1280.

(42) Kim, K.-J.; Kim, Y.-S.; Kang, W.-S.; Kang, B.-H.; Yeom, S.-H.; Kim, D.-E.; Kim, J.-H.; Kang, S.-W. Inspection of Substrate-Heated Modified PEDOT:PSS Morphology for All Spray Deposited Organic Photovoltaics. *Sol. Energy Mater. Sol. Cells* **2010**, *94*, 1303–1306.

(43) Zabihi, F.; Xie, Y.; Gao, S.; Eslamian, M. Morphology, Conductivity, and Wetting Characteristics of PEDOT:PSS Thin Films Deposited by Spin and Spray Coating. *Appl. Surf. Sci.* **2015**, *338*, 163–177.

(44) Yoon, S.-S.; Khang, D.-Y. Roles of Nonionic Surfactant Additives in PEDOT:PSS Thin Films. *J. Phys. Chem. C.* **2016**, *120*, 29525–29532.

(45) Worfolk, B. J.; Andrews, S. C.; Park, S.; Reinspach, J.; Liu, N.; Toney, M. F.; Mannsfeld, S. C. B.; Bao, Z. Ultrahigh Electrical Conductivity in Solution-Sheared Polymeric Transparent Films. *Proc. Natl. Acad. Sci. U. S. A.* **2015**, *112*, 14138–14143.

(46) Palumbiny, C. M.; Liu, F.; Russell, T. P.; Hexemer, A.; Wang, C.; Müller-Buschbaum, P. The Crystallization of PEDOT:PSS Polymeric Electrodes Probed In Situ during Printing. *Adv. Mater.* **2015**, *27*, 3391–3397.

(47) Bredas, J. L.; Street, G. B. Polarons, Bipolarons, and Solitons in Conducting Polymers. *Acc. Chem. Res.* **1985**, *18*, 309–315.

(48) Nowak, M.; Rughooputh, S. D. D. V. D. V; Hotta, S.; Heeger, A. J. Polarons and Bipolarons on a Conducting Polymer in Solution. *Macromolecules.* **1987**, *20*, 965–968.

(49) Zhang, H.; Xia, H.; Zhao, Y. Poly(Vinyl Alcohol) Hydrogel Can Autonomously Self-Heal. *ACS Macro Lett.* **2012**, *1*, 1233–1236.

(50) Sun, Y.; Xiang, N.; Jiang, X.; Hou, L. Preparation of High Tough Poly(Vinyl Alcohol) Hydrogel by Soaking in NaCl Aqueous Solution. *Mater. Lett.* **2017**, *194*, 34–37.

(51) Li, Y.; Zhang, S.; Li, X.; Unnava, V. R. N.; Cicoira, F. Highly Stretchable PEDOT:PSS Organic Electrochemical Transistors Achieved via Polyethylene Glycol Addition. *Flex. Print. Electron.* **2019**, *4*, 044004.

(52) Wool, R. P. Self-Healing Materials: A Review. *Soft Matter.* **2008**, *4*, 400–418.

(53) Grande, A. M.; Martin, R.; Odriozola, I.; van der Zwaag, S.; Garcia, S. J. Effect of the Polymer Structure on the Viscoelastic and Interfacial Healing Behaviour of Poly(Urea-Urethane) Networks Containing Aromatic Disulphides. *Eur. Polym. J.* **2017**, *97*, 120–128.

(54) Hanson, P. Alkyl Substituent Effects. Part 1. An Analysis of Alkyl Inductive Properties in Terms of Group Connectivity. *J. Chem. Soc. Perkin Trans. 2.* **1984**, *16*, 101–108.

(55) Ghittorelli, M.; Lingstedt, L.; Romele, P.; Crăciun, N. I.; Kovács-Vajna, Z. M.; Blom, P. W. M.; Torricelli, F. High-Sensitivity Ion Detection at Low Voltages with Current-Driven Organic Electrochemical Transistors. *Nat. Commun.* **2018**, *9*, 1441.

(56) Kim, K.; Park, S.; Seon, J.-B.; Lim, K.-H.; Char, K.; Shin, K.; Kim, Y. S. Patterning of Flexible Transparent Thin-Film Transistors with Solution-Processed ZnO Using the Binary Solvent Mixture. *Adv. Funct. Mater.* **2011**, *21*, 3546–3553.

Table of Contents